Journal of Biomolecular NMR, **11:** 279–288, 1998.
KLUWER/ESCOM

HMQC and HSQC experiments with water flip-back optimized for large proteins

Patrik Andersson[a,b], Bernard Gsell[b], Beat Wipf[b], Hans Senn[b] and Gottfried Otting[a,*]
[a] *Department of Medical Biochemistry and Biophysics, Karolinska Institute, Doktorsringen 9A, S-171 77 Stockholm, Sweden*
[b] *Zentrale Forschungseinheit, F. Hoffmann-La Roche AG, CH-4002 Basel, Switzerland*

Received 24 July 1997; Accepted 17 October 1997

Key words: 3D ^{15}N-HMQC-NOESY-^{15}N-HMQC, 3D NOESY-^{15}N-HMQC, DNA gyrase B, deuteration, FHMQC, FHSQC, HMQC, HSQC, ^{15}N relaxation

Abstract

An HMQC experiment is proposed, dubbed FHMQC, where water flip-back is achieved by a single water-selective pulse preceding the basic HMQC pulse sequence. The scheme is demonstrated with a ^{15}N,^{1}H-HMQC spectrum of uniformly ^{15}N/^{2}H-labelled *S. aureus* DNA gyrase B with a molecular weight of 45 kDa for the unlabelled protein. The sensitivity of the experiment is improved compared to that of an FHSQC spectrum. It is further shown that the original FHSQC experiment can be shortened by the use of bipolar gradients. Relaxation times of different ^{15}N magnetizations and coherences were measured. The new FHMQC scheme is implemented in 3D NOESY-^{15}N-HMQC and 3D ^{15}N-HMQC-NOESY-^{15}N-HMQC pulse sequences which are demonstrated with a 24 kDa fragment of uniformly ^{15}N/^{13}C/^{2}H-labelled *S. aureus* DNA gyrase B.

Introduction

HSQC (Bodenhausen and Ruben, 1980) and HMQC (Müller, 1979; Bax et al., 1983) experiments are the basic building blocks of many heteronuclear NMR experiments correlating protons and heteronuclei which are coupled by a large one-bond coupling constant. The two experiments differ by the type of coherence precessing during the evolution time t_1: while heteronuclear antiphase magnetization evolves in the HSQC experiment, mixed heteronuclear double-quantum and zero-quantum coherence evolves in the HMQC experiment. Consequently, the cross peaks in a ^{15}N,^{1}H-HSQC spectrum of a uniformly ^{15}N-labelled protein appear as singlets in the F1(^{15}N) dimension, whereas the cross peaks in a corresponding ^{15}N,^{1}H-HMQC spectrum are broadened in the F1(^{15}N) dimension due to ^{1}H-^{1}H couplings evolving during the evolution time. On the other hand, for an isolated two-spin system, the dipolar relaxation between the precessing spins becomes negligible in an HMQC experiment in the slow motional regime, where $\omega_0\tau_c \gg 1$ (ω_0: Larmor frequency; τ_c: rotational correlation time), whereas the heteronuclear single-quantum coherence evolving in an HSQC experiment relaxes more rapidly (Bax et al., 1989). Dipolar ^{1}H-^{1}H interactions, however, add a relaxation source which is more important in the HMQC than in the HSQC experiment (Swapna et al., 1997). Comparisons between the two schemes usually show better sensitivity and resolution for HSQC than HMQC spectra (Bax et al., 1990; Norwood et al., 1990). Finally, water suppression (Messerle et al., 1989; Piotto et al., 1992; Sklenář et al., 1993) and water flip-back schemes (Grzesiek and Bax, 1993; Zhang et al., 1994; Mori et al., 1995) are most readily implemented in the HSQC experiment.

Recent advances in increasing the molecular weight limit of proteins amenable to studies by high-resolution NMR spectroscopy include perdeuteration of the protein molecules. Significantly improved sensitivity and resolution has been demonstrated for

*To whom correspondence should be addressed.

the remaining amide protons of uniformly $^{15}N/^{2}H$-labelled proteins (Grzesiek et al., 1993; Yamazaki et al., 1994; Venters et al., 1995; Nietlispach et al., 1996). Since dipolar ^{1}H-^{1}H interactions are much reduced for amide protons in a perdeuterated protein and scalar ^{1}H-^{1}H couplings are removed, a $^{15}N,^{1}H$-HMQC experiment might be expected to yield significantly better sensitivity than a $^{15}N,^{1}H$-HSQC experiment, provided that a water flip-back scheme is implemented. This article presents a $^{15}N,^{1}H$-HMQC pulse sequence, the $^{15}N,^{1}H$-FHMQC sequence, featuring a simple but effective water flip-back scheme. An improvement in sensitivity over the $^{15}N,^{1}H$-HSQC experiment is demonstrated with a fragment of $^{15}N/^{2}H$-labelled *S. aureus* DNA gyrase B (residues 1–405) complexed to novobiocin. The complex has a molecular weight of 48.5 kDa (45 kDa at natural isotope abundance). As it turned out, the sensitivity advantage of the FHMQC over the FHSQC experiment was not due to decreased relaxation as demonstrated by comparable line widths in both experiments. This was confirmed by the measurement of the relaxation times of different ^{15}N magnetizations and coherences. The new $^{15}N,^{1}H$-HMQC scheme is implemented in 3D NOESY-^{15}N-HMQC (Marion et al., 1989b; Zuiderweg and Fesik, 1989) and 3D ^{15}N-HMQC-NOESY-^{15}N-HMQC (Frenkiel et al., 1990; Ikura et al., 1990) experiments and this set of experiments is illustrated with spectra recorded with a 24 kDa fragment of uniformly $^{15}N/^{13}C/^{2}H$-labelled *S. aureus* DNA gyrase B (residues 1–234) complexed to novobiocin. Finally, an improved version of the FHSQC experiment (Mori et al., 1995) is presented.

Materials and Methods

Sample preparation

Uniformly ^{15}N-labelled and >95% deuterated samples of the two N-terminal fragments of *S. aureus* DNA gyrase B comprising residues 1–405, SaGyrB(1–405), and residues 1–234, SaGyrB(1–234), were expressed in *E. coli* strain W3110 adapted to grow in a minimal medium containing 6.8 g/l KH_2PO_4, 8.7 g/l K_2HPO_4, 1.0 g/l NaCl, 1.0 g/l Na_2SO_4, 0.2 g/l $MgSO_4 \cdot 7H_2O$, 4.0 g/l Na-acetate, 0.81 g/l $^{15}NH_4Cl$, 35 mg/l thiamine-HCl, 25 mg/l citric acid monohydrate, 5 mg/l $FeCl_3 \cdot 6H_2O$, 0.5 mg/l $ZnCl_2 \cdot 4H_2O$, 0.5 mg/l $MnCl_2 \cdot 4H_2O$, 0.5 mg/l $CoCl_2 \cdot 6H_2O$, 5 mg $CaCl_2$, 0.25 mg/l $CuCl_2 \cdot 2H_2O$, 0.25 mg H_3BO_3, 0.5 mg/l $Na_2MoO_4 \cdot 2H_2O$, 0.5 mg/l $NiSO_4 \cdot 6H_2O$ and D_2O. For the production of $^{15}N/^{13}C/^{2}H$-labelled samples, $^{13}C_2$-acetate was used which was deuterated to >90% by keeping in D_2O under argon at 200 °C for 4 days. The medium was supplemented with ampicillin (100 mg/l) for the production of SaGyrB(1–234) and with ampicillin:kanamycin (100 mg/l:25 mg/l) for the production of SaGyrB(1–405). The media were sterile filtered (0.2 μm filter pore size) before use. The adapted strains were grown in shaker flasks at 37 °C and 200 rpm until the OD_{550} was about 1.0–1.2. Portions (1 ml) of these cultures were frozen at liquid nitrogen temperature for storage. Each large-scale protein expression started by inoculation of 100 ml of medium with one thawed 1 ml portion of culture. The resulting pre-culture was incubated as above until an OD_{550} of 1.0–1.2 was reached. Production cultures were initiated by inoculation of 50 ml pre-culture into 1 l of medium. Protein expression was induced by the addition of IPTG at a concentration of 119 mg/l, when an OD_{550} of 0.5–0.6 had been reached. After one doubling time, the cultures were harvested by centrifugation and the D_2O was recycled for repeated use. The procedure typically provided ∼ 2.5 g of moist cell mass per litre of medium.

The cells were resuspended in extraction buffer containing 50 mM Tris/HCl, pH 8.5, 1 mM Na_2-EDTA, 10% (w/w) saccharose, 0.05% NaN_3, 5 mM 2-mercapto-ethanol, 25 mg/l DNAse I, 25 mM $MgCl_2$, 2 mM PMSF and 5 mM diisopropylfluorophosphate. The suspension was sonicated during 5 times 30 s while kept in an ice bath, and 10% (v/v) glycerol was added subsequently. Since a major fraction of SaGyrB(1–234) appeared in inclusion bodies, the cells from SaGyrB(1–234) growths were resuspended in 8 M urea in column loading buffer containing 50 mM Tris/HCl, pH 8.5, 75 mM NaCl, 0.02% (w/w) NaN_3 and 0.025% (v/v) Tween 20, the suspension was homogenized by short bursts of sonication, and the protein was refolded (see below) before loading onto a novobiocin affinity column. In both protein preparations, the cell debris was pelleted by centrifugation, and the supernatant was filtered (0.2 μm filter pore size) and loaded onto an equilibrated novobiocin affinity column. After loading, the column was washed and equilibrated with column loading buffer, washed again with a pH gradient (from pH 7.0 to 2.3 using two glycine buffers) and re-equilibrated with column loading buffer. The fragments were eluted using 8 M urea in column loading buffer. Refolding was performed by dialysis at 4 °C against refolding buffer

containing 50 mM Tris/HCl, pH 8.5, 75 mM NaCl, 5% glycerol, 0.1% CHAPS and 0.02% NaN_3 in H_2O. After $\sim$ 12 h, the refolding buffer was changed and dialysis continued for an additional $\sim$ 4 h. The denaturation-renaturation cycle ensured the ^2H-^1H exchange of nitrogen and oxygen bound protein deuterons. Monomeric species were separated from multimeric aggregates by gel filtration (superdex 75), which also removed final traces of urea. Novobiocin was added to enhance the stability of the samples by inhibiting the self-aggregation of the SaGyrB fragments. The NMR sample of SaGyrB(1–405) was prepared at pH 8.6 by exchanging the buffer for 90% H_2O/10% D_2O, 75 mM ammonium carbonate and 0.1% CHAPS by gel filtration (superdex 75), which also removed excess novobiocin, and concentrating to a final protein concentration of 0.7 mM by ultrafiltration. The NMR sample of SaGyrB(1–234) was prepared at pH 6.6. CHAPS, $MgCl_2$ and $(NH_4)_2SO_4$ were added to the solution at pH 8.6 to final concentrations of 0.1% (w/w), 6 mM and 0.14 M, respectively, the pH was rapidly changed to 6.5 by adding deuterated acetic acid and a final pH of 6.65 was adjusted using ND_3. D_2O (8% v/v) was added and the sample was concentrated to a final protein concentration of 1 mM by ultrafiltration. Ultracentrifugation of the samples at 350 000$\times$ g, and at 8 °C for 0.5 h before placing them in NMR tubes was found to increase the stability of the samples against precipitation. NaN_3 (0.02% w/w) was present in the final NMR buffers to prevent bacterial and fungal growth. Yields were 50 mg and 9 mg of purified SaGyrB(1–234) and SaGyrB(1–405), respectively, per litre of minimal medium. The purity of the samples was assessed by reverse-phase HPLC (absorption monitored at 218 nm) and the monomeric content was verified by gel filtration (absorption monitored at 280 nm).

NMR spectroscopy

NMR spectra were recorded at a ^1H frequency of 600 MHz on a Bruker DMX-600 NMR spectrometer and processed using the NMRPipe/NMRDraw program package (Delaglio et al., 1995). The time domain data were multiplied by cosine or cosine-squared window functions before Fourier transformation to avoid truncation effects.

Results and Discussion

FHSQC and FHMQC experiments

Figure 1 shows the pulse sequence of the FHSQC experiment (Mori et al., 1995), our modified FHSQC experiment and the FHMQC experiment. The main differences between the original FHSQC experiment (Figure 1A) and our modified version (Figure 1B) are the omission of the gradients after the second and before the third 90°(^1H) pulse and the use of bipolar gradients during the evolution time t_1. Omitting the delays shortens the experiment, minimizing signal losses due to relaxation of the longitudinal two-spin order present during those delays. In the original FHSQC experiment of Mori et al. (1995), the gradients (G_2 in Figure 1A) serve to defocus the transverse water magnetization to suppress radiation damping during the evolution time t_1 and to refocus it again after t_1. In this way, the following 90°(^1H) pulse can flip the water magnetization back to the z-axis and radiation damping is suppressed during t_1 which would otherwise compromise the water flip-back for longer evolution times, leading to more scrambled water magnetization after the Watergate sequence and therefore increased saturation transfer to protein protons. The gradients must not be too strong to avoid loss of magnetization by diffusion. In our modified version of the FHSQC experiment, weak bipolar gradients (Sklenář, 1995) are used to prevent radiation damping during t_1 (Figure 1B).

The water flip-back in the FHMQC experiment is effected by a single selective 90° pulse applied to the water magnetization with the same phase as the following hard 90°(^1H) excitation pulse. The inverted water magnetization is subsequently flipped back to its equilibrium position by the following 180°(^1H) pulse. The gradient after the hard 90°(^1H) pulse prevents the recovery of equilibrium water magnetization by radiation damping. The protein magnetization defocused by the gradient after the hard 90°(^1H) pulse is refocused before acquisition by a second gradient of the same strength and duration. A more intense gradient pulse preceding the pulse sequence serves to defocus any residual transverse water magnetization from previous scans which could otherwise compromise the quality of the water suppression.

On current 600 MHz NMR spectrometers, a single gradient pulse suppresses radiation damping of inverted water magnetization for a time period of about 30 ms (Otting and Liepinsh, 1995a,b). Thus, the water flip-back effected by the 180°(^1H) pulse is still good

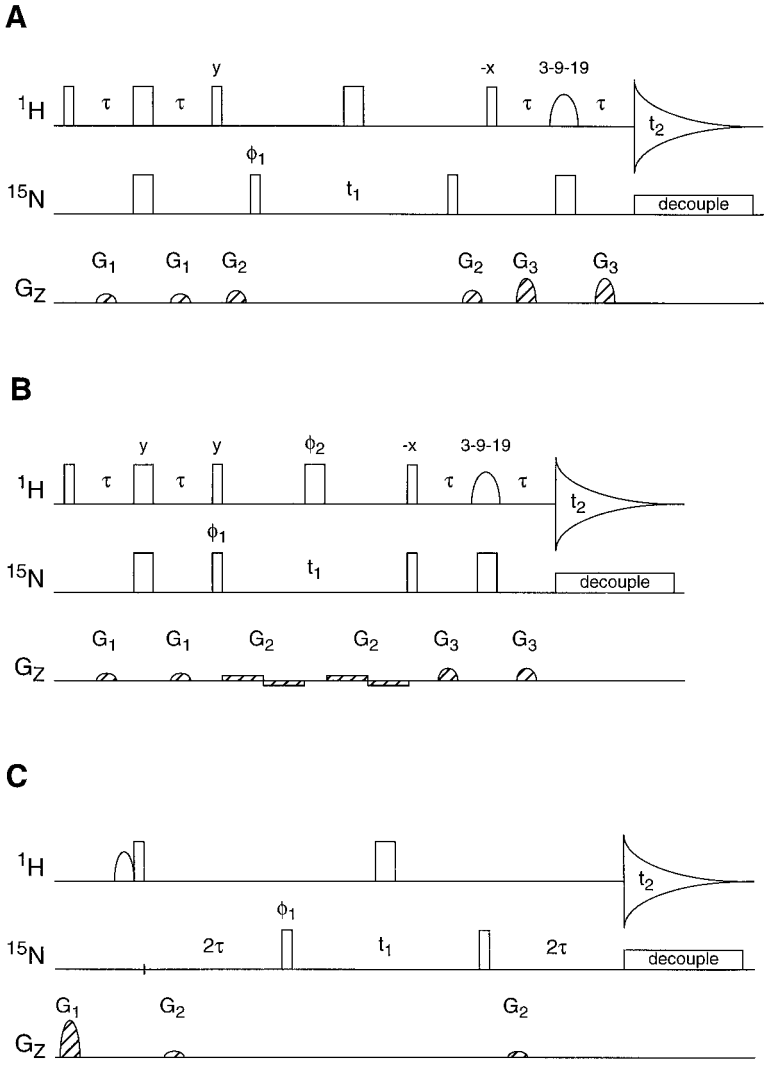

Figure 1. Pulse sequences of the original FHSQC experiment (A), a modified version thereof (B) and the fast HMQC experiment with water flip-back (FHMQC) (C). The ^{1}H carrier frequency is set at the water resonance. Narrow (wide) rectangular pulses represent flip angles of 90° (180°), and bell-shaped pulses represent selective pulses. All pulses, except where noted and the 3-9-19 selective pulse (Sklenář, 1995), are applied with phase x. Pulsed field gradients are sine-bell shaped with a duration of 1.0 ms, followed by an eddy current recovery delay of 100 μs. Bipolar gradients during t_1 are rectangular. The States-TPPI scheme (Marion et al., 1989a) is applied to all ^{15}N pulses preceding t_1 (Hammarström and Otting, 1994). $\tau = 1/(4^1 J_{HN})$. (A) Original FHSQC experiment (Mori et al., 1995). Phase cycle: ϕ_1 = x,−x; receiver phase =x,−x. Gradient strengths: $G_{1,2,3}$ = 3.5, 5.0 and 10.0 G/cm, respectively. (B) Modified FHSQC experiment. Phase cycle: ϕ_1 = 2(x,−x); ϕ_2 =y,y,−y,−y; receiver phase = 2(x,−x). $G_{1,2,3}$ = 1.5, 0.5 and 3.5 G/cm. (C) FHMQC experiment. Water flip-back is achieved by a single selective 90° pulse. Same phase cycle as in (A). $G_{1,2}$ = 15 and 2.5 G/cm.

for t_1 values of about 60 ms. For longer t_{1max} values or systems with faster radiation damping (Talluri and Wagner, 1996), the water magnetization is no longer perfectly aligned with the z-axis right after the 180° pulse, but radiation damping during the residual t_1 period helps to return the water magnetization to its equilibrium position before the start of the acquisition period t_2. Alternatively, radiation damping during t_1 could be suppressed altogether by the use of bipolar gradients as in the modified FHSQC experiment (Figure 1B).

It is an advantage of the FHMQC pulse sequence of Figure 1C that the water-selective 90° pulse is applied while the protein magnetization is in equilibrium. Thus, a relatively long, selective pulse (John et al., 1992; Shen and Lerner, 1995; Mori et al., 1996)

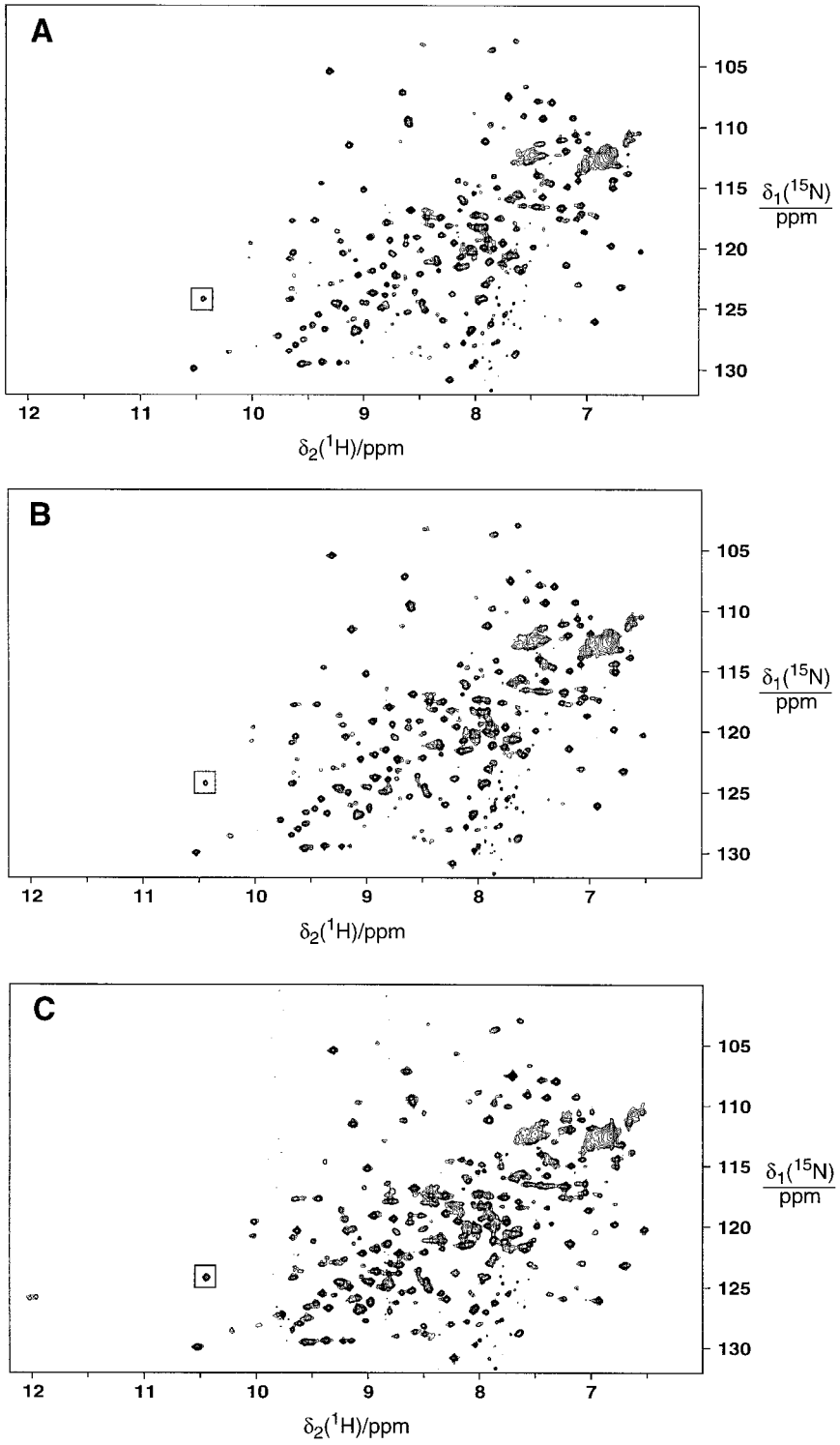

Figure 2. ^{15}N-^{1}H correlations recorded with a 0.7 mM aqueous solution of uniformly ^{15}N/^{2}H-labelled SaGyrB(1–405) at 25 °C, pH 8.6, using the experimental schemes of Figure 1. Recording, processing and plotting parameters were identical for all three spectra, using $\tau = 2.5$ ms, $t_{1max} = 81.6$ ms, $t_{2max} = 104.8$ ms, a recycle delay of 1.2 s and a total experimental time per spectrum of 1.5 h. Broadband decoupling: ^{15}N, 1.14 kHz GARP (Shaka et al., 1985); ^{2}H, 1.25 kHz Waltz-16 (Shaka et al., 1983) during t_1 and t_2. (A) ^{15}N,^{1}H-FHSQC spectrum recorded with the pulse sequence of Figure 1A. (B) ^{15}N,^{1}H-FHSQC spectrum recorded with the pulse sequence of Figure 1B. (C) ^{15}N,^{1}H-FHMQC spectrum recorded with the pulse sequence of Figure 1C. The water-selective 90° pulse was shaped as an element in Seduce decoupling (McCoy and Müller, 1992) and applied with a duration of 2.0 ms.

Table 1. Overview of relaxation times $T_{1,2}$ of different ^{15}N product operators in SaGyrB(1-405)

Operator	$T_{1,2}$[a]	Pulse sequence used[b]	Reference
N_x	33 ± 6 ms	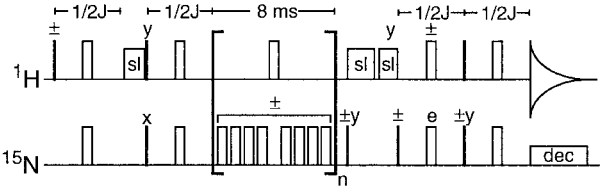	Skelton et al. (1993) Farrow et al. (1994)
N_z	1.7 ± 0.2 ms	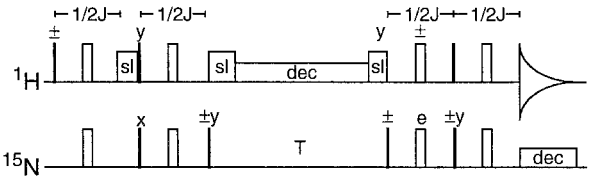	Skelton et al. (1993)
N_xH_x	21 ± 1 ms	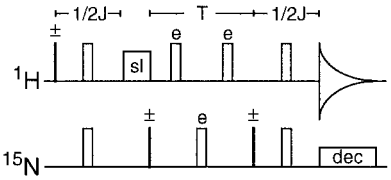	
N_xH_x	22 ± 2 ms	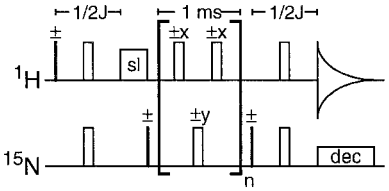	
N_zH_z	110 ± 30 ms	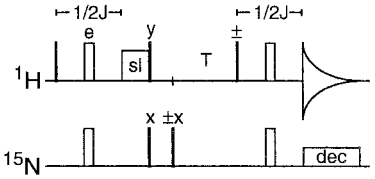	Boyd et al. (1990)

[a] Relaxation times $T_{1,2}$ were determined by fitting the function $I = I_0 \exp(-T/T_{1,2})$ to the signal intensities in spectra recorded with different relaxation delays T. The listed $T_{1,2}$ values are averages over relaxation times determined at six different ^1H chemical shifts in the ranges 7.4–7.8 and 8.6–9.0 ppm, avoiding signals from mobile residues. Standard deviations reflect the spread of the $T_{1,2}$ values determined at the different amide proton chemical shifts.

[b] Schematic representations of the pulse sequences used. Narrow (wide) pulses represent flip angles of 90° (180°). Spin-lock pulses were used with durations of 0.5, 1, and 2 ms. Unless otherwise noted, pulses were applied with phase x. Independently phase alternated pulses are identified by a ± sign. e denotes EXORCYCLE. The relaxation delay is labelled T or composed of n times the pulse element in square brackets. Pulses in brackets were phase cycled together. Equally spaced relaxation delays were used: 0.001, 0.251, ..., 2.001 s (N_z), 8, 16, ..., 56 ms (N_x), 1, 41, ..., 241 ms (N_zH_z), 1, 9, ..., 49 ms (N_xH_x).

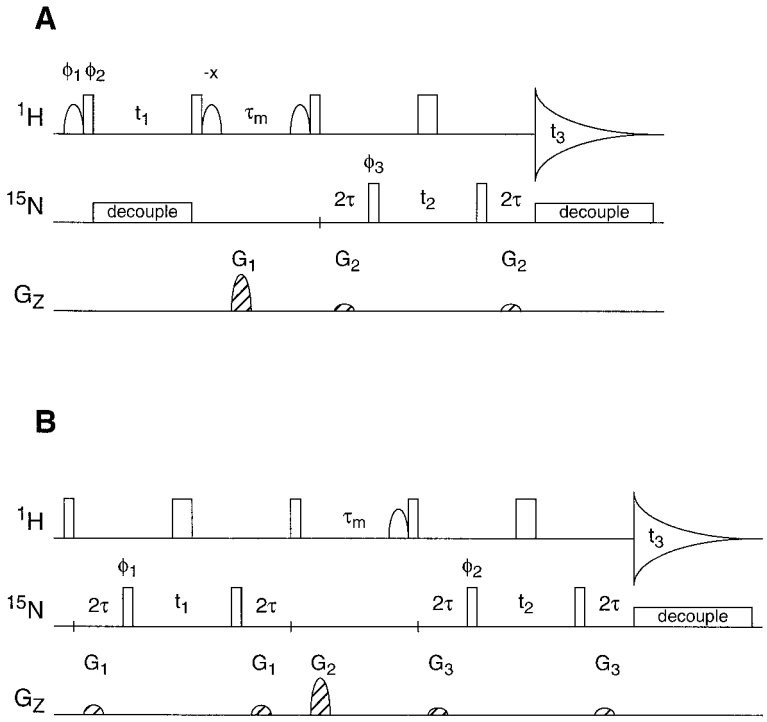

Figure 3. Pulse sequences of 3D NOESY-^{15}N-HMQC (A) and 3D ^{15}N-HMQC-NOESY-^{15}N-HMQC with water flip-back (B). The ^{1}H carrier frequency is set at the water resonance. All pulses are applied with phase x unless indicated otherwise. Pulsed field gradients are sine-bell shaped with a duration of 1.0 ms. The States-TPPI scheme (Marion et al., 1989a) is applied to all ^{15}N pulses preceding t_1 (Hammarström and Otting, 1994). $\tau = 1/(4^1J_{HN})$. (A) 3D NOESY-^{15}N-HMQC. Phase cycle: $\phi_1 = -\phi_2 = -x,-x,x,x$; $\phi_3 = 2(x,-x)$; receiver =x,−x,−x,x. Gradient strengths: $G_{1,2} = 15.0$ and 2.5 G/cm. Quadrature detection in the indirect ^{1}H (^{15}N) dimension is achieved by incrementing the phases of all ^{1}H (^{15}N) pulses preceding the respective evolution periods according to the States (States-TPPI) scheme (States et al., 1982; Marion et al., 1989a). With the ^{1}H carrier at the water resonance, the axial peaks appear at F1 = $\delta(H_2O)$, i.e. half the spectral region of the amide protons can be folded without interference with axial peaks. (B) 3D ^{15}N-HMQC-NOESY-^{15}N-HMQC. Phase cycle: ϕ_1 =x,x,−x,−x; $\phi_2 = 2(x,-x)$; receiver =x,−x,−x,x. Gradient strengths: $G_{1,2,3} = 4.0$, 15.0 and 2.5 G/cm. Quadrature detection is achieved in both indirect dimensions by States-TPPI applied to all ^{15}N pulses preceding the respective evolution times.

can be used without much penalty in sensitivity, allowing the observation of cross peaks close to the water resonance, provided that care is taken to suppress radiation damping during the selective pulse (Otting and Liepinsh, 1995a,b; Böckmann and Guittet, 1996). In contrast, the selectivity of the Watergate schemes (Piotto et al., 1992; Sklenář et al., 1993) is limited by the short time interval available in the reverse INEPT step of the HSQC experiments, resulting in excitation profiles with a relatively broad zero at the water frequency and problems to observe amide protons close to the water resonance. The widely used '3-9-19' sequence (Sklenář et al., 1993) decreases the intensities of amide proton resonances even at frequencies far from the water resonance.

The pulse schemes of Figure 1 were tested with a sample of ^{15}N/^{2}H-labelled SaGyrB(1–405). As expected, the ^{15}N,^{1}H-FHSQC spectrum recorded with the modified pulse sequence of Figure 1B (Figure 2B) is most similar to the ^{15}N,^{1}H-FHSQC spectrum recorded with the originally proposed pulse sequence of Figure 1A (Figure 2A). A quantitative comparison of the peak heights showed that the modified FHSQC scheme afforded, on average, 1.09-fold higher signal intensities, with a standard deviation of 0.13.

The water suppression in the ^{15}N,^{1}H-FHMQC experiment (Figure 2C) was not as good as in the FHSQC spectra, but sufficient to allow a receiver gain setting that did not compromise the sensitivity. Straightforward baseline correction completely removed the dispersive wings of the residual water signal in the spectral region of interest. Figure 2C shows that the signal intensities were improved for almost all cross peaks, not only for resonances near 6.5 and 12 ppm which were incompletely refocused by the 3-9-19 sequence in the experiments of Figures 2A and B. On

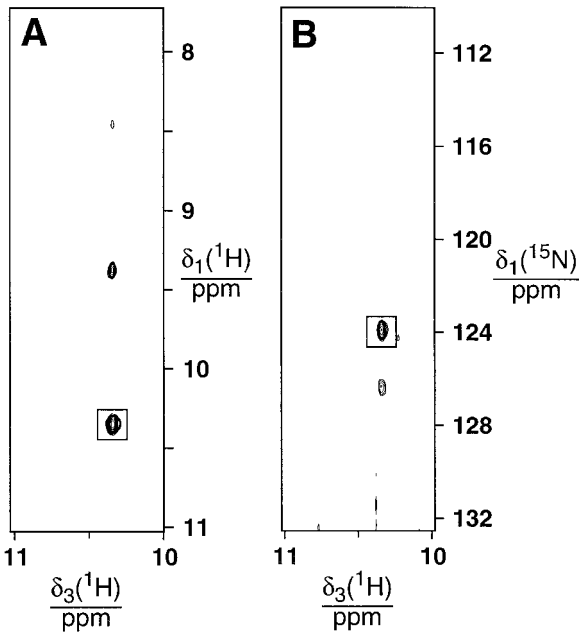

Figure 4. Two-dimensional slices from 3D NOESY-^{15}N-HMQC (A) and 3D ^{15}N-HMQC-NOESY-^{15}N-HMQC (B) spectra recorded with a 1 mM aqueous solution of uniformly ^{15}N/^{13}C/^{2}H-labelled SaGyrB(1–234) at 35 °C, pH 6.6, using the experimental schemes of Figures 3A and B, respectively. The slices were taken at $\delta_2(^{15}N)$= 123.9 ppm, showing the diagonal peak and cross peaks of the amide group identified by a box in the spectra of Figure 2. Experimental parameters: τ = 2.5 ms; τ_m = 200 ms; recycle delay 0.9 s. Broadband decoupling: ^{15}N, 1.14 kHz GARP (Shaka et al., 1985); ^{2}H, 1.25 kHz Waltz-16 (Shaka et al., 1983) during t_1 and t_2; ^{13}C, 1.0 kHz Seduce (McCoy and Müller, 1992) during t_1, t_2 and t_3. The ^{13}C carrier frequency was placed midway between the carbonyl and α-carbon resonances and the pulse train was modulated by a cosine function for simultaneous irradiation of carbonyl and α-carbons. The water-selective 90° pulses were shaped as an element in Seduce decoupling (McCoy and Müller, 1992) and applied with a duration of 2.0 ms. (A) 3D NOESY-^{15}N-HMQC spectrum. t_{1max} = 23.3 ms, t_{2max} = 27.2 ms, t_{3max} = 104.8 ms, total experimental time 46 h. (B) 3D ^{15}N-HMQC-NOESY-^{15}N-HMQC spectrum. t_{1max} = t_{2max} = 31.7 ms, t_{3max} = 104.8 ms, total experimental time 62 h.

average, the peak heights increased by more than 35% compared to the FHSQC spectrum of Figure 2A, with a standard deviation of 29% for 240 peaks evaluated.

The line widths measured in the ^{15}N dimension of the FHMQC spectrum were comparable to those measured in the FHSQC spectra, but not narrower. Thus, the improved sensitivity seems to be more a consequence of the fewer pulses present in the FHMQC experiment (Norwood et al., 1990; van Zijl et al., 1996) than due to more favourable relaxation properties during the evolution time t_1. For a deeper analysis, we measured the relaxation times of different ^{15}N magnetizations and coherences.

^{15}N relaxation measurements

The relaxation measurements were performed with the ^{15}N/^{2}H-labelled sample of SaGyrB(1–405) under the conditions used to record the spectra of Figure 2. Relaxation rates were measured for longitudinal and transverse ^{15}N magnetization, N_z and N_x, respectively, longitudinal two-spin order N_zH_z, and two-spin coherence N_xH_x, where N and H denote the spin operators of amide nitrogens and amide protons, respectively, and transverse operators are denoted as N_x and H_x irrespective of whether they represent an x or a y component in a Cartesian coordinate system. The measurements were conducted as one-dimensional ^{1}H-detected experiments, evaluating the signal intensities in different regions of the amide proton spectrum as a function of the relaxation delay. The signal intensities were fitted by single exponential decays, assuming similar relaxation rates for different amide groups with overlapping ^{1}H chemical shifts. The validity of this assumption was supported by the fact that similar relaxation rates were obtained from different regions of the amide proton spectrum. The only exception was the spectral region between 7.8 and 8.6 ppm, where the measured relaxation times were apparently predominated by residues of increased mobility.

Table 1 gives an overview of the relaxation times measured and the pulse sequences used. The ratio of the ^{15}N T_1 and T_2 relaxation times indicates a rotational correlation time (Skelton et al., 1993) of the SaGyrB(1–405) sample of about 23 ns. The relaxation times of N_xH_x coherences were measured in two ways, once with a minimum number of 180° refocusing pulses and once with a train of 180° pulses providing a spin-locking effect on both ^{15}N and ^{1}H spins. Both measurements yielded similar T_2 relaxation times which were shorter than for in-phase ^{15}N magnetization N_x (Table 1). Antiphase (N_xH_z) and in-phase (N_x) magnetization alternates during the evolution time of the HSQC experiment, resulting in an average relaxation time that is somewhat shorter than that of pure N_x magnetization. Consequently, similar line widths may be expected in HMQC and HSQC experiments, as observed experimentally. Based on the relaxation time of the longitudinal two-spin order N_zH_z, one would predict about 2% improved sensitivity for the shortened FHSQC scheme of Figure 1B compared to the original FHSQC experiment (Figure 1A).

3D NOESY-HMQC and 3D HMQC-NOESY-HMQC experiments with water flip-back

The FHMQC experiment can readily be implemented in 3D NOESY-HMQC and HMQC-NOESY-HMQC experiments (Figure 3). The NOESY-HMQC pulse sequence (Figure 3A) uses three water-selective 90° pulses, the first two applied with opposite phase as the associated hard 90°(^{1}H) pulses, whereas the same phase is used for the third selective pulse as for the following hard pulse. In this way, the water magnetization is in its equilibrium position during the evolution period t_1 and during most of the mixing time τ_m, rendering the pulse sequence suitable for use with short mixing times.

The HMQC-NOESY-HMQC pulse sequence (Figure 3B) provides water flip-back already with a single water-selective 90° pulse which is applied with the same phase as the following hard 90°(^{1}H) pulse. The water magnetization is longitudinal during the mixing time τ_m, enabling the use of short mixing times. As in the NOESY-HMQC sequence of Figure 3A, the quality of water suppression is assured by an intense gradient pulse during the mixing time.

Experimental spectra using the pulse sequences of Figure 3 were recorded with a sample of ^{15}N/^{13}C/^{2}H-labelled SaGyrB(1–234). Figure 4 shows slices from the 3D NOESY-^{15}N-HMQC spectrum (Figure 4A) and the 3D ^{15}N-HMQC-NOESY-^{15}N-HMQC spectrum (Figure 4B) containing the diagonal peak of the amide group which appears in the ^{15}N,^{1}H-HSQC and HMQC spectra at the position marked by a box (Figure 2). The cross peak of this amide group is markedly affected by the non-uniform excitation profile in the HSQC spectra recorded with the 3-9-19 WATERGATE scheme (Figures 2A and B). In the 3D spectra recorded with the HMQC scheme, intense cross peaks can be observed with this amide group.

Conclusions

The HMQC experiment with water flip-back can be performed with short repetition rate without much penalty in sensitivity, because the water magnetization is returned to its equilibrium position by the end of the pulse sequence and not suppressed by saturation. In analogy to the acronym FHSQC, we propose the name FHMQC for the HMQC experiment with water flip-back. The FHMQC experiment is more sensitive than the FHSQC experiment for large, uniformly ^{15}N-labelled, perdeuterated proteins. It is therefore an attractive building block in multidimensional heteronuclear NMR experiments.

Acknowledgements

P.A. acknowledges an SSF fellowship within the Strategic Research in Structural Biology programme. Financial support from the Swedish Natural Science Research Council (Project 10161) is gratefully acknowledged.

References

Bax, A., Griffey, R.H. and Hawkins, B.L. (1983) *J. Magn. Reson.*, **55**, 301–315.

Bax, A., Kay, L.E., Sparks, S.W. and Torchia, D.A. (1989) *J. Am. Chem. Soc.*, **111**, 408–409.

Bax, A., Ikura, M., Kay, L.E., Torchia, D.A. and Tschudin, R. (1990) *J. Magn. Reson.*, **86**, 304–318.

Böckmann, A. and Guittet, E. (1996) *J. Biomol. NMR*, **8**, 87–92.

Bodenhausen, G. and Ruben, D.J. (1980) *Chem. Phys. Lett.*, **69**, 185–189.

Boyd, J., Hommel, U. and Campbell, I.D. (1990) *Chem. Phys. Lett.*, **175**, 477–482.

Delaglio, F., Grzesiek, S., Vuister, G., Zhu, G., Pfeifer, J. and Bax, A. (1995) *J. Biomol. NMR*, **6**, 277–293.

Farrow, N.A., Muhandiram, R., Singer, A.U., Pascal, S.M., Kay, C.M., Gish, G., Shoelson, S.E., Pawson, T., Forman-Kay, J.D. and Kay, L.E. (1994) *Biochemistry*, **33**, 5984–6003.

Frenkiel, T., Bauer, C., Carr, M.D., Birdsall, B. and Feeney, J. (1990) *J. Magn. Reson.*, **90**, 420–425.

Grzesiek, S., Anglister, J., Ren, H. and Bax, A. (1993) *J. Am. Chem. Soc.*, **115**, 4369–4370.

Grzesiek, S. and Bax, A. (1993) *J. Am. Chem. Soc.*, **115**, 12593–12594.

Hammarström, A. and Otting, G. (1994) *J. Magn. Reson.*, **A109**, 246–249.

Ikura, M., Bax, A., Clore, G.M. and Gronenborn, A.M. (1990) *J. Am. Chem. Soc.*, **112**, 9020–9022.

John, B.K., Plant, D., Webb, P. and Hurd, R.E. (1992) *J. Magn. Reson.*, **98**, 200–206.

Marion, D., Ikura, M., Tschudin, R. and Bax, A. (1989a) *J. Magn. Reson.*, **85**, 393–399.

Marion, D., Kay, L.E., Sparks, S.W., Torchia, D.A. and Bax, A. (1989b) *J. Am. Chem. Soc.*, **111**, 1515–1517.

McCoy, M.A. and Müller, L. (1992) *J. Am. Chem. Soc.*, **114**, 2108–2112.

Messerle, B.A., Wider, G., Otting, G., Weber, C. and Wüthrich, K. (1989) *J. Magn. Reson.*, **85**, 608–613.

Mori, S., Abeygunawardana, C., Johnson, M.O. and van Zijl, P.C.M. (1995) *J. Magn. Reson.*, **B108**, 94–98.

Mori, S., Abeygunawardana, C., van Zijl, P.C.M. and Berg, J.M. (1996) *J. Magn. Reson.*, **B110**, 96–101.

Müller, L. (1979) *J. Am. Chem. Soc.*, **101**, 4481–4484.

Nietlispach, D., Clowes, R.T., Broadhurst, R.W., Ito, Y., Keeler, J., Kelly, M., Ashurst, J., Oschkinat, H., Domaille, P.J. and Laue, E.D. (1996) *J. Am. Chem. Soc.*, **118**, 407–415.

Norwood, T.J., Boyd, J., Heritage, J.E., Soffe, N. and Campbell, I.D. (1990) *J. Magn. Reson.*, **87**, 488–501.

Otting, G. and Liepinsh, E. (1995a) *J. Biomol. NMR*, **5**, 420–426.
Otting, G. and Liepinsh, E. (1995b) *J. Magn. Reson.*, **B107**, 192–196.
Piotto, M., Saudek, V. and Sklenář, V. (1992) *J. Biomol. NMR*, **2**, 661–665.
Shaka, A.J., Keeler, J., Frenkiel, T. and Freeman, R. (1983) *J. Magn. Reson.*, **52**, 335–338.
Shaka, A.J., Barker, P.B. and Freeman, R. (1985) *J. Magn. Reson.*, **64**, 547–552.
Shen, J. and Lerner, L.E. (1995) *J. Magn. Reson.*, **A112**, 265–269.
Skelton, N.J., Palmer III, A.G., Akke, M., Kördel, J., Rance, M. and Chazin, W.J. (1993) *J. Magn. Reson.*, **B102**, 253–264.
Sklenář, V., Piotto, M., Leppik, R. and Saudek, V. (1993) *J. Magn. Reson.*, **A102**, 241–245.
Sklenář, V. (1995) J. Magn. Reson., **A114**, 132–135.
States, D.J., Haberkorn, R.A. and Ruben, D.J. (1982) *J. Magn. Reson.*, **48**, 286–292.
Swapna, G.V.T., Rios, C.B., Shang, Z. and Montelione, G.T. (1997) *J. Biomol. NMR*, **9**, 105–111.
Talluri, S. and Wagner, G. (1996) *J. Magn. Reson.*, **B112**, 200–205.
Van Zijl, P.C.M., Hwang, T.L., Johnson, M.O. and Garwood, M. (1996) *J. Am. Chem. Soc.*, **118**, 5510–5511.
Venters, R.A., Huang, C., Farmer, B.T., Trolard, R., Spicer, L.D. and Fierke, C.A. (1995) *J. Biomol. NMR*, **5**, 339–344.
Yamazaki, T., Lee, W., Arrowsmith, C.H., Muhandiram, D.R. and Kay, L.E. (1994) *J. Am. Chem. Soc.*, **116**, 11655–11666.
Zhang, O.W., Kay, L.E., Olivier, J.P. and Forman-Kay, J.D. (1994) *J. Biomol. NMR*, **4**, 845–858.
Zuiderweg, E.R.P. and Fesik, S.W. (1989) *Biochemistry*, **28**, 2387–2391.